Polymer Journal (2018) 50:375–380
https://doi.org/10.1038/s41428-018-0022-1

ORIGINAL ARTICLE

Metastable interface formation in isotactic poly(methyl methacrylate)/alumina nanoparticle mixtures

Kazuki Matsuura[1] · Yasuhiro Matsuda[1] · Shigeru Tasaka[1]

Received: 26 September 2017 / Revised: 22 December 2017 / Accepted: 26 December 2017 / Published online: 13 February 2018

Abstract

The interface structures of isotactic poly(methyl methacrylate) (it-PMMA)/alumina nanoparticle (Al_2O_3; ~40 nm) mixtures from tetrahydrofuran (THF) solutions were investigated by X-ray diffraction (XRD), Fourier transform infrared (FT-IR) spectroscopy, and differential scanning calorimetry (DSC). The mixtures of it-PMMA can form two amorphous phases with different crystallinities depending on casting conditions from THF. These structures are metastable and have different activation energies for crystal nucleus formation. The polymer interface on Al_2O_3 particles changes into a crystallizable amorphous phase with a trans-gauche-rich chain conformation.

Introduction

In 1958, Fox et al. reported that the synthesis of stereoregular poly(methyl methacrylate) (PMMA) leads to three types of crystallizable polymers [1]. The three polymer types have different X-ray diffraction patterns and properties. The three types are isotactic polymers, syndiotactic polymers, and isotactic-syndiotactic block copolymers. Fox et al. also reported that it is possible to crystalize isotactic poly(methyl methacrylate) (it-PMMA). It should be noted that it-PMMA forms helical crystals with five monomeric units per turn [2, 3].

Because of this, the crystallization behavior of it-PMMA has received much attention. Kumaki et al. made it possible to obtain molecular images of various polymer structures by tapping-mode AFM for Langmuir–Blodgett films [4]. Crystallization of some polymers can be promoted by the proper solvent or temperature [5]. The crystallization of it-PMMA is a very slow process and is achieved by annealing at a high temperature for several days or weeks in a melt-cast or solution-cast it-PMMA film [6]. The crystalline samples can be obtained by freeze-extracting it-PMMA from a PEG solution and annealing at a temperature near the glass transition temperature for 48 h [7].

It-PMMA has also received considerable attention due to its ability to a form double helical structure [8]. By forming complexes with solvents, it-PMMA is known to self-aggregate to form double helical structures with obvious crystalline characteristics [9, 10]. Its aggregation behavior is strongly dependent on the degree of stereoregularity, solvent and temperature [11]. It-PMMA forms a double helical structure upon crystallization, and peaks appear at $2\theta = 8°$ and 31° in the X-ray diffraction pattern [12]. It-PMMA also forms two-dimensional folded chain crystals composed of double-stranded helices [13]. The structure and properties of a polymer generally change at interfaces with other materials. Physical properties at the surfaces and interfaces of polymer thin films are actively being studied [14, 15]. Glass transition temperatures of the interface region changes due to the strong interactions between the polymer and substrate [16]. Tannenbaum et al. reported high density and conformational changes of PMMA at the interface through various measurements of composites prepared by mixing PMMA and various metal oxide particles [17–19]. The glass transition temperatures of composite samples of PMMA and Al_2O_3 are lower than that of pure PMMA [20–22].

PMMA is widely used as composites with inorganic fillers. Metal alkoxides [23–25] or colloidal inorganic nanoparticles [26–28] are generally used for studies on PMMA/inorganic oxide materials. However, the structure and physical properties of the polymer at the alumina

✉ Yasuhiro Matsuda
matsuda.yasuhiro@shizuoka.ac.jp

[1] Department of Applied Chemistry and Biochemical Engineering, Shizuoka University, 3-5-1 Johoku, Naka-ku, Hamamatsu 432-8561, Japan

nanoparticle interfaces in the composite are not fully understood.

In this paper, we discuss the interface polymer structures of it-PMMA/Al_2O_3 samples. By using samples with high nanoparticle contents, the interfacial structure of it-PMMA with a thickness of 100 nm thick can be characterized by X-ray diffractometry (XRD), Fourier transform infrared spectroscopy (FT-IR), and differential scanning calorimetry (DSC).

Experimental procedure

Materials

Isotactic poly(methyl methacrylate) (it-PMMA, it = 97.1%) was purchased from Aldrich. The glass transition temperature (T_g) of the as-received it-PMMA was measured to be 35 °C. Tetrahydrofuran (THF) was used to dissolve it-PMMA. Alumina nanoparticles were spherical and were purchased from Kanto Chemical. The average particle diameter and density of γ-alumina (Al_2O_3) were reported by the supplier to be 41.4 nm and 3.6 g/cm^3, respectively.

Measurements

XRD patterns were obtained with a MiniFlex 300 (Rigaku, Tokyo, Japan). The measurements were performed using CuKα radiation as the X-ray source, a tube voltage of 30 kV, a tube current of 30 mA, a scan range of 4–40°, and a scanning speed of 2° min^{-1}. The XRD pattern of the alumina particles was subtracted from the pattern of the mixed samples to isolate the structural information of the polymer.

FT-IR spectra were obtained using an FT/IR-4100 (JASCO, Tokyo, Japan) with a diamond cell (Type DX2010, Sumitomo Electric Hard Metal, Tokyo, Japan). The resolution, scan number and measured wavenumbers were 2, 500, and 400–4000 cm^{-1}, respectively.

DSC curves were obtained using DSC-60 (Shimadzu, Tokyo, Japan). The nitrogen flow rate, heating rate and measurement temperature range were 150 ml min^{-1}, 20 °C min^{-1}, and −40 to 200 °C, respectively.

Preparation of isotactic poly(methyl methacrylate)/Al_2O_3 nanoparticles mixture

THF-cast samples

The mixed samples of it-PMMA and alumina nanoparticles were prepared as follows. Alumina nanoparticles were heated for 2 h at 800 °C to remove residual water and hydroxide groups from the nanoparticles using a muffle furnace (FO100, Yamato Scientific, Tokyo, Japan) before mixing. The amount of residual water was measured to be less than 1.5 wt% by thermogravimetry. It-PMMA was dissolved in THF to obtain solution with 0.1 g/ml, and nanoparticles were added to this solution. This sample was mixed for 20 min in a mortar, cast on an aluminum substrate at room temperature and dried under vacuum. No residual solvent was detected in these samples by FT-IR analysis. Furthermore, no endothermic peak was observed at the boiling point of THF by DSC. No endothermic peaks were observed in any samples.

Melt-cast samples

The melt-cast samples were prepared in the same manner as the THF-cast samples, then heated at a temperature (160 °C) sufficiently higher than melting temperature for 2 min. These samples were cooled to room temperature to form a thin film, showed the same physical properties as received it-PMMA.

Annealed samples

The annealed samples were prepared by heating the mixed samples at 60 °C for 48 h using a vacuum drying apparatus (DN43H, Yamato Scientific Co., Tokyo, Japan).

Results and discussion

Figure 1 shows the XRD patterns of the melt-cast samples (it-PMMA bulk, it-PMMA/Al_2O_3 (30), and it-PMMA/Al_2O_3 (50)). The numbers in parentheses indicate the weight percentages of the nanoparticles in the samples. The curves in the figure were calculated by subtracting the pattern of the nanoparticles from those of the mixed samples [29, 30]. Broad peaks typical of amorphous it-PMMA are observed. The melt-cast sample of it-PMMA bulk shows a main peak at $2\theta = 13°$. Comparing the results of each sample, the main peak shifts to higher angles with an increase of Al_2O_3 nanoparticles. In the it-PMMA/Al_2O_3 (50) sample, the peak position of the main peak was 1° higher than that of the bulk sample, and a new broad peak appeared around $2\theta = 8°$. Because the peak position changed beyond an experimental error, the addition of Al_2O_3 induced an amorphous structure slightly different from that of bulk PMMA. The crystals of it-PMMA are reported to have peaks at approximately $2\theta = 7°$, 14°, and 28° [12]. Because peaks also appear around these angles for the crystals of it-PMMA, the appearance of a broad peak at this angle means that a structure capable of crystallization is formed at the interface [12].

Figure 2 shows the DSC curves of the melt-cast samples (it-PMMA bulk and it-PMMA/Al_2O_3 mixtures). The DSC curve for it-PMMA bulk shows a glass transition at 35 °C, while the DSC curves for the it-PMMA/Al_2O_3 mixtures show glass transitions and a broad change at 0 °C. Ash et al. reported that PMMA/Al_2O_3 nanocomposites have a glass transition temperature 25 °C lower than PMMA [20–22]. In addition, Fujii et al. reported that the glass transition temperature of PMMA decreases on the surface [31]. The broad change detected at 0 °C in Fig. 2 may be derived from the structure of PMMA at the Al_2O_3 interphase structure.

Here, we assume that all the Al_2O_3 nanoparticles dispersed in the samples are spheres with a diameter of 41.4 nm. Further, the densities of the it-PMMA in a bulk state and the interface have no significant difference. The ratio of XRD pattern area of interphase to the peak area of it-PMMA bulk corresponds to the weight ratio of it-PMMA interphase and bulk. The thickness of the interphase of it-PMMA/Al_2O_3 (50) is estimated to be about 5–10 nm. The interphase also becomes thicker with an increase Al_2O_3. This means the existence of chains restricted by the surface of Al_2O_3 [29].

In fact, there is a high possibility that the nanoparticles are aggregated in the samples. Therefore, it is expected that the interface structure is formed around not all the nanoparticles, and that the thickness of the interface becomes thicker than 10 nm in the sample with aggregates.

Figure 3 shows the XRD patterns of the melt-cast sample (it-PMMA bulk) and the THF-cast samples (it-PMMA bulk, it-PMMA/Al_2O_3 (30) and it-PMMA/Al_2O_3 (50)). The melt-cast sample of it-PMMA has a main peak at $2\theta = 13°$. In contrast, the THF-cast samples of it-PMMA have peaks at $2\theta = 7$, 14, and 28° [12], and the peaks are broader. Therefore, the amorphous structure of it-PMMA is changed by THF. Furthermore, the peaks shift to higher angles, and the shape of the peak at approximately $2\theta = 23$–30° also changes with the addition of alumina nanoparticles. From the results of each sample, the peak of it-PMMA bulk (THF-cast) at $2\theta = 14°$ shifts to higher angles with an increase of Al_2O_3 nanoparticles. This change is similar to that of the melt-cast sample. Therefore, it was found that the amorphous structure of it-PMMA was changed by THF, and it-PMMA forms a novel amorphous structure at interfaces with alumina nanoparticles.

Figure 4 shows the DSC curves of the melt-cast sample (it-PMMA bulk) and the THF-cast samples (it-PMMA bulk and it-PMMA/Al_2O_3 mixtures). The DSC curve for the melt-cast sample of it-PMMA bulk shows a glass transition at 35 °C and no melting peak. In contrast, the THF-cast sample of it-PMMA bulk shows a glass transition around 0 °C. The decrease in the glass transition temperature is also observed for the mixed samples (THF-cast). The glass transition temperature of PMMA surface decreases due to adsorptions and contact with different materials [32, 33]. Therefore, the THF-cast sample (it-PMMA bulk) may form a metastable amorphous structure.

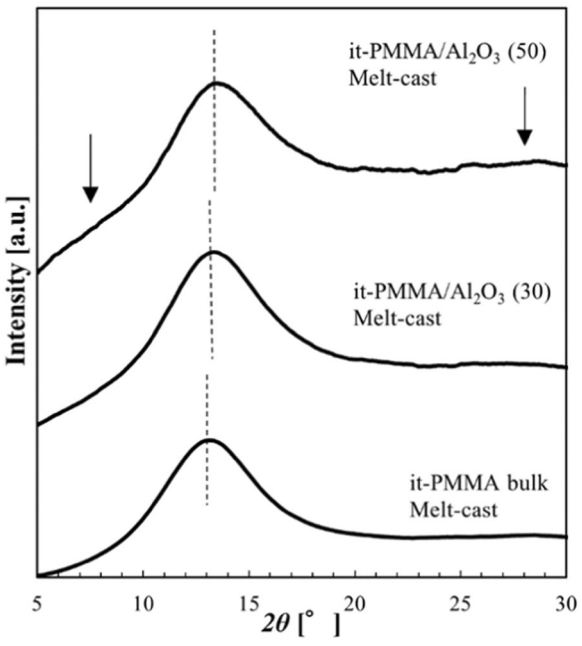

Fig. 1 XRD patterns of melt-cast samples (it-PMMA bulk, it-PMMA/Al_2O_3 (30) and it-PMMA/Al_2O_3 (50)). The curves in the figure were calculated by subtracting the pattern of the nanoparticles from those of the mixed samples

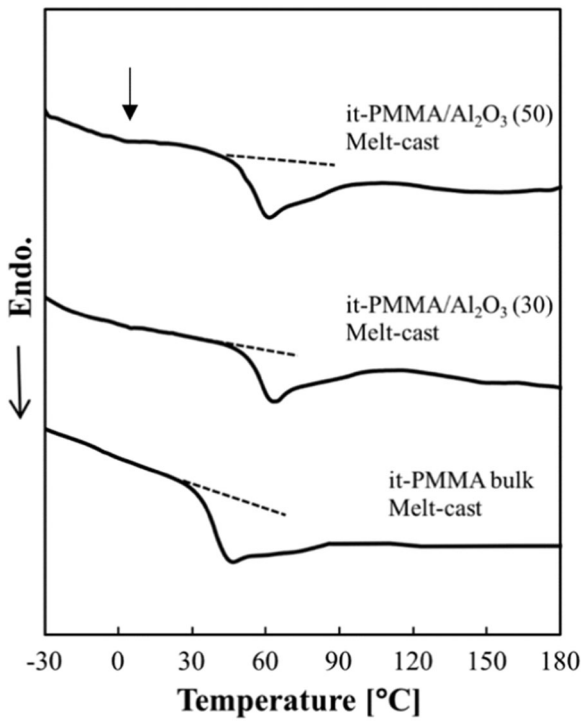

Fig. 2 DSC curves for melt-cast samples (it-PMMA bulk and it-PMMA/Al_2O_3 samples). (2nd scan data) The heating rate was 20 °C/min

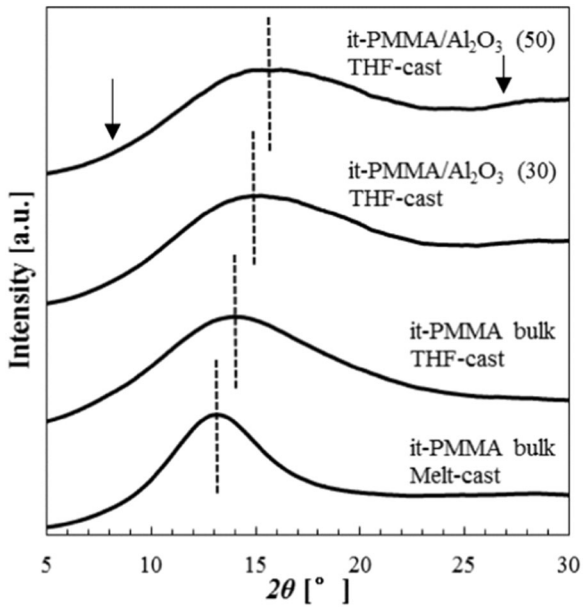

Fig. 3 XRD patterns of melt-cast sample (it-PMMA bulk) and THF-cast samples (it-PMMA bulk, it-PMMA/Al_2O_3 (30) and it-PMMA/Al_2O_3 (50)). The curves in the figure were calculated by subtracting the pattern of the nanoparticles from those of the mixed samples

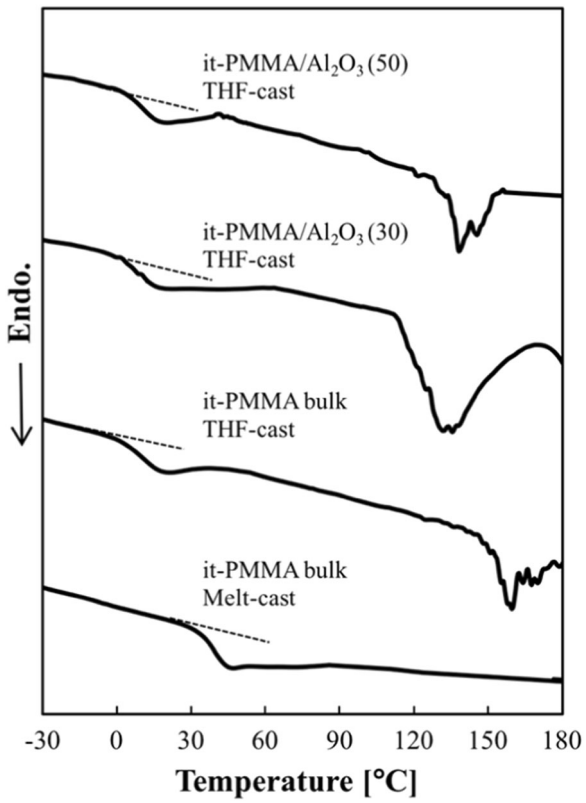

Fig. 4 DSC curves for melt-cast sample (it-PMMA bulk) and THF-cast samples (it-PMMA bulk and it-PMMA/Al_2O_3 samples). (1st scan data) The heating rate was 20 °C/min

On the other hand, a melting peak was observed at 150 °C for the it-PMMA bulk sample (THF-cast) and 130 °C for the it-PMMA/Al_2O_3 mixed samples. As will be shown later, annealing the THF-cast sample at a temperature slightly higher than T_g produces crystals. During the heating scan of the samples, it is possible that the it-PMMA bulk and the mixed samples generated small crystals due to an effect similar to what is seen in heat treatment.

Figure 5 shows the FT-IR spectra of the air dried samples (it-PMMA bulk and it-PMMA/Al_2O_3 mixtures) in the 1000–1800 cm^{-1} range. The peak at 1065 cm^{-1} does not depend on the conformation of the main chain. Therefore, the FT-IR spectrum in Fig. 5 was normalized using the peak at 1065 cm^{-1}. The insert shows around the peak top at 1130–1220 cm^{-1} [1]. The absorption peaks at 1195, 1150, and 1065 cm^{-1} are attributed to the anti-symmetric vibrations of C–O–C, stretching vibrations of C–O coupled with skeletal vibrations, and skeletal vibrations of the main chain, respectively [34]. It is known that the absorption peak at 1150 cm^{-1} increases as the content of trans–trans conformations decreases in favor of the trans-gauche conformations. In the upper right of Fig. 5, the IR spectrum of the peak at approximately 1165 cm^{-1}, from which conformational information can be obtained, is shown in detail. The peak of it-PMMA/Al_2O_3 was larger than the peak of it-PMMA bulk. Therefore, the structure of it-PMMA/Al_2O_3 consists of a larger fraction of chains in trans-gauche conformations (helical).

On the other hand, it is known that it-PMMA crystallizes due to the influence of solvent and temperature. It-PMMA is crystallized by heat treatment for a long time at a temperature slightly higher than the glass transition temperature, and as a result of the crystallization, a peak appears in the X-ray diffraction pattern, and a melting peak appears in the DSC curve [7].

Figure 6 shows the XRD patterns of the it-PMMA bulk samples (melt-cast) annealed at 60 °C, which is near the glass transition of amorphous bulk it-PMMA (melt-cast). A peak caused by crystallization was observed at $2\theta = 8.5°$ in the it-PMMA bulk sample (THF-cast and annealed). There was no obvious crystal peak for the it-PMMA/Al_2O_3 mixed samples, but that shape of the peak at $2\theta = 5–10°$ is distinctly different from that of the amorphous single peak of bulk it-PMMA. Gradual crystallization may also have occurred at the interface in this sample. The main peak shifted to higher angles with the addition of alumina nanoparticles in the THF-cast samples in Fig. 3. On the other hand, the peak in Fig. 6 only became sharper, and showed no significant change in the peak angles.

Therefore, when the it-PMMA is annealed and the it-PMMA/Al_2O_3 mixture is cast from THF, a crystal structure can be formed in the bulk material or at the interface, meaning the amorphous structure partially crystallizes from a nucleus in a helical conformation. Additionally, the

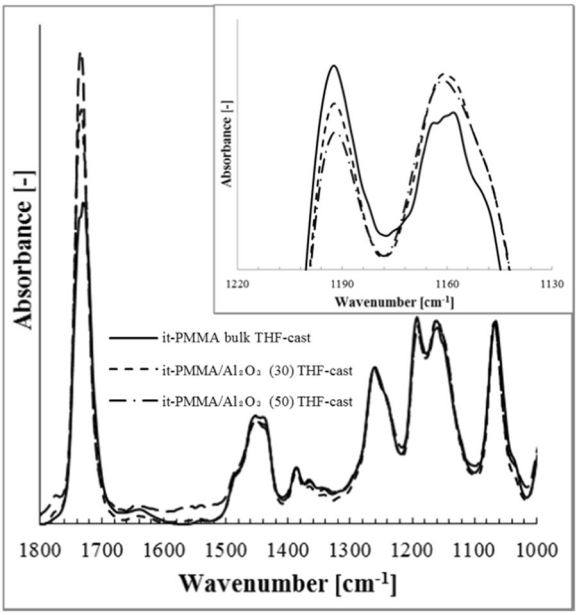

Fig. 5 IR spectra in the 1000–1800 cm^{-1} region of THF-cast samples (it-PMMA bulk, it-PMMA/Al_2O_3 (30) and it-PMMA/Al_2O_3 (50))

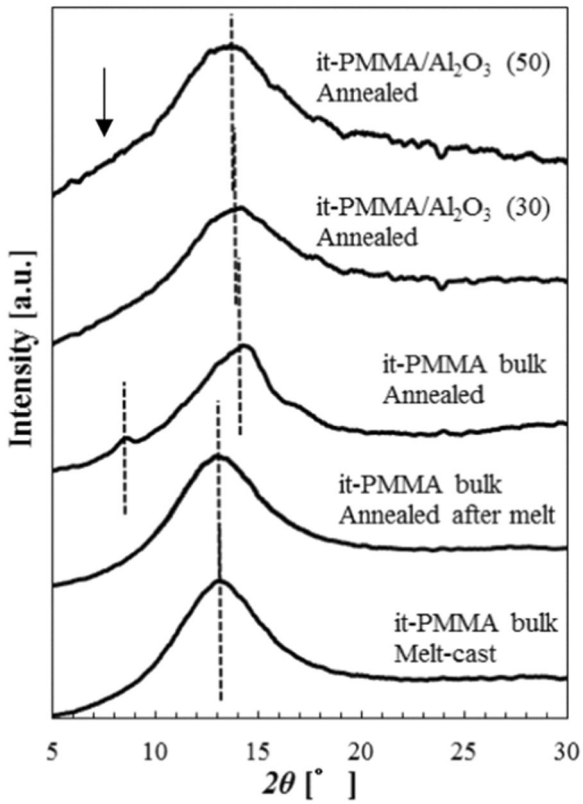

Fig. 6 XRD patterns of it-PMMA bulk (melt-cast, annealed after melt) and annealed samples (it-PMMA bulk, it-PMMA/Al_2O_3 (30) and it-PMMA/Al_2O_3 (50)) The curves in the figure were calculated by subtracting the pattern of the nanoparticles from those of the mixed samples

conformation changes very little at the interface even in the annealed sample.

Furthermore, once it-PMMA is molten at 160 °C and cooled to form a non-crystallizable amorphous, this thermally stable structure is never changed by annealing.

From the experimental results so far, the amorphous structure of the it-PMMA changes by THF casting, it-PMMA has a crystallizable amorphous structure, and the conformation of the chain is stable on the surface of alumina nanoparticles. Therefore, during annealing for a long time at a temperature near the glass transition temperature, both the it-PMMA bulk sample and the it-PMMA/Al_2O_3 mixed samples will crystallize.

The following structural changes could be observed in the it-PMMA. A double helical structure can be formed in the samples cast from THF or annealed. The double helical structure is immobilized at the interface with the alumina nanoparticles. In a molten sample with Al_2O_3, strong interaction between it-PMMA and Al_2O_3 prevents it-PMMA forming the helical structure.

Conclusion

The metastable structures of it-PMMA at the interfaces with Al_2O_3 nanoparticles were examined using XRD measurements, FT-IR measurements and DSC thermograms. The amorphous it-PMMA structure is changed by THF. A new amorphous structure is also formed at the alumina nanoparticle interface. Furthermore, it-PMMA forms crystal nuclei and crystallizes by annealing at temperatures near the glass transition temperature. However, when annealing is not performed, crystal nuclei cannot be formed at the alumina nanoparticle interfaces, and a novel amorphous structure different from the bulk state is formed. We believe that it-PMMA crystallizes while forming a double helical structure, its structure is retained at the alumina nanoparticle interface, and melting causes the double helix to unravel.

Compliance with ethical standards

Conflict of interest The author declares that they have no competing interests.

References

1. Fox TG, Garrett BS, Goode WE, Gratch S, Kincaid JF, Spell A, Stroupe JD. Crystalline polymers of methyl methacrylate. J Am Chem Soc. 1958;80:1768–69.
2. Stroupe JD, Hughes RE. The structure of crystalline poly-(methyl methacrylate). J Am Chem Soc. 1958;80:2341–42.
3. Coiro VM, De Santis P, Liquori AM, Mazzarella L. The molecular conformation of isotactic poly (methyl methacrylate). J Polym Sci Part C. 1969;16:4591–96.

4. Kumaki J. Observation of polymer chain structures in two-dimensional films by atomic force microscopy. Polym J. 2016;48:3–14.
5. Kamei D, Ajiro H, Hongo C, Akashi M. Solvent effects on isotactic poly(methyl methacrylate) crystallization and syndiotactic poly(methacrylic acid) incorporation in porous thin films prepared by stepwire stereocomplex assembly. Langmuir. 2009;25:280–85.
6. de Boer A, van Ekenstein G, O, R, A, Challa G. Crystallization of isotactic poly(methyl methacrykate) from the melt. Polymer. 1975;16:930–32.
7. Dongshan Z, Liang L, Bo C, Qin C, Yun L, Gi X. Metastable isotactic poly(methyl methacrylate) prepared by freeze-extracting solutions in poly(ethylene glycol). Macromolecules. 2004;37:4744–47.
8. Kusanagi H, Tadokoro H, Chatani Y. Double strand helix of isotactic poly(methyl methacrylate). Macromolecules. 1976;9:531–32.
9. Könnecke K, Rehage G. Crystallization and stereo association of stereoregular PMMA. Colloid Polym Sci. 1981;259:1062–69.
10. Spěváček J, Schneider B. Aggregation of stereoregular poly (methyl methacrylates). Adv Colloid Interface Sci. 1987;27:81–50.
11. Bistac B, Schultz J. Influence of polymer/solvent acid-base interactions on the aggregation of stereoregular PMMA. Macromol Chem Phys. 1997;198:531–35.
12. Christofferson AJ, Yiapanis G, Ren JM, Qiao GG, Satoh K, Kamigaito M, Yarovsky I. Molecular mapping of poly(methyl methacrylate) super-helix stereocomplexes. Chem Sci. 2015;6:1370–78.
13. Kumaki J, Kawauchi T, Yashima E. Two-dimensional folded chain crystals of a synthetic polymer in a Langmuir-Blodgett film. J Am Chem Soc. 2005;127:5788–89.
14. Forrest JA, Dalnoki-Veress K. The glass transition in thin polymer films. Adv Colloid Interface Sci. 2001;94:167–95.
15. Tanaka K. Glass transition of polymers in confined systems. Kobunshi Ronbunshu. 2006;63:539–47.
16. Forrest JA, Dalnoki-Veress K, Stevens JR, Dutcher JR. Effect of free surfaces on the glass transition temperature of thin polymer films. Phys Rev Lett. 1996;77:2002–5.
17. Tannenbaum R, Zubris M, David K, Ciprari D, Jacob K, Jasiuk I, Dan N. FTIR characterization of the reactive interface of cobalt oxide nanoparticles embedded in polymeric matrices. J Phys Chem B. 2006;110:2227–32.
18. Ciprari D, Jacob K, Tannenbaum R. Characterization of polymer nanocomposite interphase and its impact on mechanical properties. Macromolecules. 2006;39:6565–73.
19. Konstadinidis K, Thakkar D, Chakraborty A, Potts WL, Tannenbaum R, Tirrell M, Evans FJ. Segment level chemistry and chain conformation in the reactive adsorption of poly(methyl methacrylate) on aluminum oxide surfaces. Langmuir. 1992;8:1307–17.
20. Ash BJ, Rogers DF, Wiegand CJ, Schadler LS, Siegel RW, Benicewicz BC, Apple T. Mechanical properties of Al_2O_3/polymethylmethacrylate nanocomposites. Polym Comp. 2002;23:1014–25.
21. Ash BJ, Siegel RW, Schadler LS. Glass-transition temperature behavior of alumina/PMMA nanocomposites. J Polym Sci B. 2004;42:4371–83.
22. Ash BJ, Siegel RW, Schadler LS. Mechanical behavior of alumina/poly(methyl methacrylate) nanocomposites. Macromolecules. 2004;37:1358–69.
23. Coltrain BK, Landry CJT, O'Reilly JM, Chamberlain AM, Rakes GA, Sedita JS, Kelts LW, Landry MR, Long VK. Role of trialkoxysilane functionalization in the preparation of organic-inorganic composites. Chem Mater. 1993;5:1445–55.
24. Chen WC, Lee SJ. Synthesis and characterization of poly(methyl methacrylate)-silica hybrid optical thin films. Polym J. 2000;32:67–72.
25. Huang ZH, Qiu KY. The effects of interactions on the properties of acrylic polymers/silica hybrid materials prepared by the in situ sol-gel process. Polymer. 1997;38:521–26.
26. Sunkara HB, Jethmalani JM, Ford WT. Composite of colloidal crystals of silica in poly(methyl methacrylate). Chem Mater. 1994;6:362–64.
27. Joseph R, Zhang S, Ford WT. Structure and dynamics of a colloidal silicapoly(methyl methacrylate) composite by ^{13}C and ^{29}Si MAS NMR spectroscopy. Macromolecules. 1996;29:1305–12.
28. Yu YY, Chen CY, Chen WC. Synthesis and characterization of organic–inorganic hybrid thin films from poly(acrylic) and monodispersed colloidal silica. Polymer. 2003;44:593–1.
29. Matsuura K, Matsuda Y, Tasaka S. Structure of polyacrylate/nanoparticle interfaces. IET Micro Nano Lett. 2017;12:667–69.
30. Fukatsu H, Kuno M, Matsuda Y, Tasaka S. Surface effect of silica nanoparticles with different size on thermotropic liquid crystalline polyester composites. World J Nano Sci Eng. 2014;4:5–41.
31. Fujii Y, Akabori K, Tanaka K, Nagamura T. Chain conformation effects on molecular motions at the surface of poly(methyl methacrylate) films. Polym J. 2007;39:928–34.
32. Smith LSA, Schmitz V. The effect of water on the glass transition temperature of poly(methyl methacrylate). Polymer. 1988;29:1871–78.
33. Atarashi H, Fujii Y, Yamazaki D, Hino M, Morita H, Tanaka K. Density distributions of poly (methyl methacrylate) thin films in non-solvents. Koubunshi Ronbunshu. 2011;68:608–15.
34. Tretinnikov ON. Selective accumulation of functional groups at the film surfaces of stereoregular poly(methyl methacrylate)s. Langmuir. 1997;13:2988–92.